

AXIAL FLOW COMPRESSORS

Fluid Mechanics and Thermodynamics

J. H. HORLOCK

M.A., PH.D., A.M.I.MECH.E., A.F.R.AE.S.

*University Lecturer in Engineering
Cambridge University*

LONDON
BUTTERWORTHS SCIENTIFIC PUBLICATIONS
1958

UTC 2018 001

BUTTERWORTHS PUBLICATIONS LTD.
88 KINGSWAY, LONDON, W.C.2

AFRICA: BUTTERWORTH & CO. (AFRICA) LTD.
DURBAN: 33/35 Beach Grove

AUSTRALIA: BUTTERWORTH & CO. (AUSTRALIA) LTD.
SYDNEY: 8 O'Connell Street
MELBOURNE: 430 Bourke Street
BRISBANE: 240 Queen Street

CANADA: BUTTERWORTH & CO. (CANADA) LTD.
TORONTO: 1367 Danforth Avenue

NEW ZEALAND: BUTTERWORTH & CO. (AUSTRALIA) LTD.
WELLINGTON: 49/51 Ballance Street
AUCKLAND: 35 High Street

©

Butterworths Publications Limited
1958

*Printed and bound in Great Britain by
The Garden City Press Limited
Letchworth, Hertfordshire*

UTC 2018 002

Chapter 2

TWO-DIMENSIONAL CASCADES: THEORETICAL ANALYSES OF PERFORMANCE

2.0 INTRODUCTION

IN THE development of the highly efficient modern axial flow compressor, the study of the two-dimensional flow through cascades of aerofoils has played an important part. For compressors in which the ratio of hub radius to tip radius is large, the flow through a row of blades may be considered as approximately two dimensional, as radial velocities will always be small and the cascade is a close model of the flow in the machine. For compressor stages of lower hub-tip ratio, blades will be twisted along the length to accommodate the radial variations in flow, but information from two-dimensional cascades is still useful to the designer in analysing the flow through each section of the blading in such stages.

Several attempts have been made to analyse the two-dimensional potential flow through cascades of aerofoils, and these are detailed in this chapter. Much experimental testing of cascades has also been undertaken, and several empirical correlations of the test data have been made. These correlations are given in Chapter 3.

The nomenclature and the basic aerodynamic terminology used in both aspects of this cascade work are tabulated below.

2.1 CASCADE PERFORMANCE

2.1.1 Cascade nomenclature and terminology

Figure 2.1, which is reproduced from Howell's early paper⁸¹ on cascade theory and performance, shows the standard nomenclature, related to aerofoils in cascade, which is used in both Chapters 2 and 3.

In British practice the cascade aerofoil is built up around a basic camber line which is usually a circular or parabolic arc. The profiles used in British designs are termed the *C* series of aerofoils⁸² and Table 2.1 gives thickness versus length along the chord line for one of these aerofoils (*C1*).

Cascade geometry is then decided completely by the aerofoil specification, the stagger (γ) and the space-chord ratio (s/l). The aerofoil nomenclature is best illustrated by an example.

12C4/35 P30 denotes an aerofoil for which the maximum thickness-chord ratio (t/l) is 12 per cent, C4 denotes the base profile, 35 is the camber angle in degrees, P denotes a parabolic arc camber line, and 30 is the percentage of the chord from the leading edge where maximum camber occurs.

CASCADES: EXPERIMENTAL WORK

nearer the 'negative' stalling ('choking') limit at design operating conditions, in order to obtain more flexibility off-design.

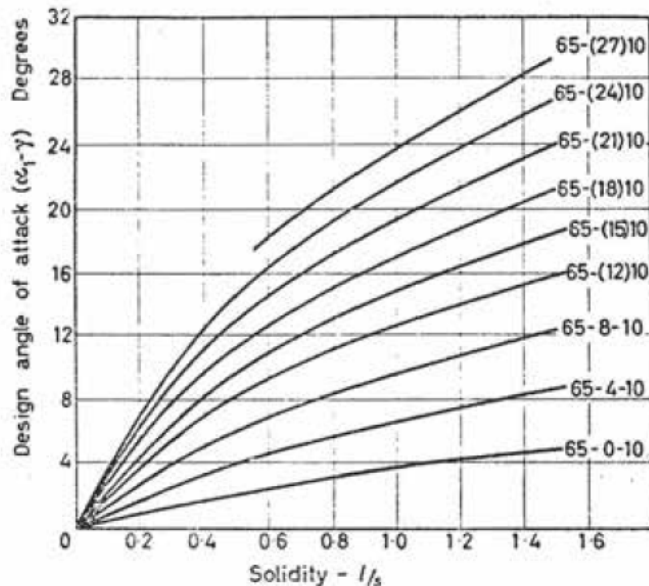


Figure 3.10. Design angles of attack ($\alpha_1 - \gamma$) for NACA 65-series. (L. J. Herrig, J. C. Emery and J. R. Erwin⁴⁷. Courtesy NACA)

3.4 CORRELATIONS OF THE EFFECT OF MACH NUMBER

As the entry Mach number to a given cascade is increased at a given incidence so the pressure rise across the cascade falls off. Figure 3.11 shows the beginning of this drop in pressure rise at the *critical* Mach number M_{nc} (when the maximum local Mach number in the cascade reaches unity). At the *maximum* entry Mach number M_{nmax} the cascade is fully choked. Howell has attempted to correlate the drops in efficiency and deflection in terms of a relation between the operating Mach number M_n and the critical and maximum Mach numbers $[(M_n - M_{nc}) / (M_{nmax} - M_{nc})]$ (Figure 3.12).

Using this correlation, curves similar to Figure 3.11 may be drawn for each incidence. Figure 3.13 shows how M_{nc} and M_{nmax} vary with the throat area-inlet area ratio, which may be calculated for a given cascade at each incidence.

Thus for a given cascade operating lines may be plotted on graphs of $\alpha_1 - M_n$, showing the limit of efficient operation (positive and negative stalling) (Figure 3.14). Within the envelope the cascade is unstalled. Such graphs are important in the analysis of blade flutter.

The work of Carter²⁰ and Andrews⁴ indicates in general that efficient operation at higher Mach numbers can be obtained by moving the maximum